

Thermal Σ - Δ Modulator: Anemometer Performance Analysis

Will R. M. Almeida¹, Georgina M. Freitas¹, Ligia S. Palma³, Sebastian Y.C. Catunda², Raimundo C. S. Freire¹, Francisco F. Santos¹, Amauri Oliveira³, Hassan Aboushady⁴

¹Universidade Federal de Campina Grande, Unidade Academica de Engenharia Eletrica, Campina Grande - PB, Brazil.

²Universidade Federal do Maranhao, Departamento de Engenharia de Eletricidade, Sao Luis – MA, Brazil.

³Universidade Federal da Bahia, Departamento de Engenharia Eletrica, Salvador – BA, Brazil.

⁴University of Paris VI, Pierre & Marie Curie, LIP6/ASIM Laboratory, 75252 Paris, France

Email: {willalmeida, rcsfreire, ffsantos}@dee.ufcg.edu.br, geo_maciel@hotmail.com, catunda@dee.ufma.br, {ligia, amauri}@ufba.br, Hassan.Aboushady@lip6.fr.

Abstract – In this paper we propose a feedback architecture with a thermoresistive sensor, based on the thermal sigma-delta principle to realize digital measurement of physical quantities that interacts with the sensor: temperature, thermal radiation, fluid speed. This architecture uses a 1-bit sigma-delta modulator for which a considerable part of the conversion functions is performed by a thermoresistive sensor. The sensor is modelled using the electrical equivalence principle and the constant temperature measurement method is applied. We present an analysis of the system performance, in terms of frequency response and system measurement resolution, of a 1-bit first-order Σ - Δ thermal modulator. It is shown that the system performance depends on the system oversampling ratio (OSR) and on the system transfer function pole and zero, which in turn, depends on the thermal and physical sensor characteristics and on the system operating conditions. This system is proposed as anemometer.

Keywords – Thermoresistive sensor, Anemometer, Sigma-delta modulation, Constant temperature architecture, Microsensors.

I. INTRODUCTION

The classical architectures of hot-wire anemometer are based on the equivalence principle for which the sensing element is a thermoresistive sensor, the estimated output is an analog signal and the configuration used is an Wheatstone bridge with the sensor placed in one of its branches in a constant temperature arrangement. Other Wheatstone bridge configurations use pulse width modulation in the feedback loop. The simplicity and robustness of sigma-delta A/D converters makes this category of A/D converters an excellent candidate for smart sensor applications [1, 2]. Realizing both functional and economical characteristics of integrating sensor and signal processing functions on a chip sets a challenge of complexity and component tolerance on the integrated circuit design. An easier alternative is the use of sigma-delta configurations with the sensor as part of the feedback loop.

A mono-bit first-order thermal Σ - Δ modulator, as shown in Figure 1, was proposed as anemometer, which is based on the electric equivalence principle with the sensor operating at a constant temperature [3]. This fluid speed measurement system directly transforms the physical signal into its

equivalent digital form and may be integrated with a microsensor.

In the proposed mono-bit first-order Σ - Δ modulator architecture, the sum and integration operations are performed by the sensor. In this paper, the proposed anemometer system performance is analyzed and discussed.

II. BACKGROUND DEFINITIONS

The dynamic heat equation for a thermoresistive sensor can be expressed by [3-5]:

$$P_e + \alpha HS = hS(T_s - T_f) + mc \frac{dT_s}{dt} \quad (1)$$

where, αSH is the incident thermal radiation absorbed by the sensor, $P_e = I_s^2 R_s$ is the electrical power delivered to the sensor, h is the heat transfer coefficient referred to the sensor surface area S , T_s is the sensor temperature, T_f is the fluid temperature, m is the sensor mass, c is the sensor specific heat.

The sensor temperature, T_s , can be given by:

$$T_s = \frac{1}{mc} \int (\alpha HS + I_s^2 R_s - hS(T_s - T_f)) dt \quad (2)$$

Figure 1 shows the block diagram of a first-order sigma-delta modulator. The summing and integrating blocks are in evidence, showing the similarity with (2).

The idea of including the microsensor into a 1-bit first-order sigma-delta loop comes from the mentioned similarity and from the fact that the sensor temperature response curve leads to an almost exponential function in response to a squared current step for small steps amplitudes. Thus,

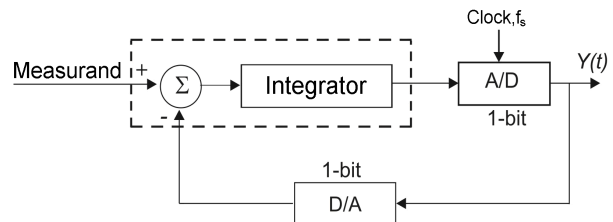


Figure 1. Block diagram of a first-order sigma-delta modulator.

considering that the sampling frequency, f_s , is much greater than the sensor linear transfer function pole frequency, this exponential can be approximated by an integration function, for which the gain is the exponential function initial slope. Considering that the step response for an ideal integrator and for the exponential are almost coincident until 10% of the exponential time constant, some studies were carried out analyzing the small signals model for the sigma-delta converters, employed for the measurement of thermal radiation and environment temperature [6]. Based on these studies and assuming that H is equal to zero, we propose a structure based on sigma-delta modulation for estimation fluid speed (ϑ). Hence, T_s , can be expressed by:

$$T_s = \frac{1}{mc} \int I_s^2 R_s - hS(T_s - T_f) dt \quad (3)$$

The thermoresistive microsensor used has a positive temperature coefficient, PTC. The thermal behavior mathematical model of the PTC is given by:

$$R_s = R_o [1 + \beta(T_s - T_f)] \quad (4)$$

where R_o is the sensor resistance at 0 °C and β is the thermal coefficient, which is a function of the sensor material.

Rewritten (3), considering the substitutions: I_s^2 for Y_s and $h = a + b\vartheta^n$ and assuming the condition of static thermal balance, the sensor squared current (Y_s), can be expressed by:

$$Y_s = \frac{1}{R_s} [S(a + b\vartheta^n)(T_s - T_f)] \quad (5)$$

Thus, assuming that the sensor temperature is kept almost constant, ϑ can be evaluated from the knowledge Y_s as:

$$\vartheta = \left\{ \frac{1}{b} \left[\frac{Y_s R_s}{S(T_s - T_f)} - a \right] \right\}^{1/n} \quad (6)$$

A. Continuous Current modulator Σ - Δ model

Figure 2 shows the block diagram the continuous current (CC) sigma-delta modulator behavioural model with the thermoresistive microsensor working as the summing and integrating component. The fluid speed $\vartheta(t)$ and the sensor squared current, $Y_s(t)$, are the input signals whereas the sensor temperature, T_s , is the output signal. The sensor substitutes the original 1-bit first-order Σ - Δ modulator sum and integration functions.

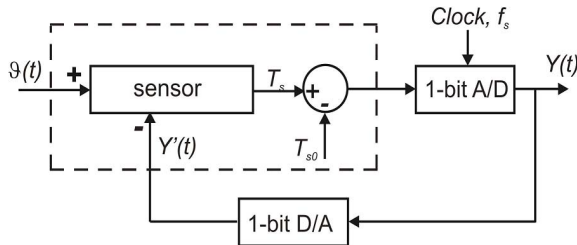


Figure 2. Block diagram of the continuous signal Σ - Δ modulator model.

As the sensor is designed to operate at constant temperature, a comparator is included into feedback loop to verify sensor temperature. If sensor temperature is greater than a reference value the 1-bit D/A (quantizer) generates a “1” bit at the modulator output. This bit, introduced in modulator feedback path, reduces the sensor current reducing also the sensor temperature. If sensor temperature is smaller than the reference value the 1-bit D/A generates a “-1” bit at the modulator output. This bit introduced in modulator feedback path increases the sensor current increasing also the sensor temperature.

B. Pulsed current Σ - Δ modulator model.

Figure 3 shows the block diagram of the pulsed-current (PC) sigma-delta behavioural model. The squared current Y_s , from the continuous-signal model, is replaced by a pulsed current $I_{s(PWM)}$, generated by the PWM block, which is proportional to Y_s . The PWM generates a pulsed current with only two pulse widths, one pulse width for quantizer output “1” and another pulse width for quantizer output “-1”. In the thermal equilibrium state, the pulse width has a theoretical value of 50% of the PWM period (T_{PWM}). The fluid speed information is now in the pulse width, which has a nonlinear relationship with the former.

III. PERFORMANCE ANALYSIS

A performance analysis for the continuous current system is carried out in this section, in terms of the system frequency response and measurement resolution.

A. Continuous Signal System Transfer Function.

Figure 4 shows the block diagram of a sampled version in the s-domain of the proposed architecture, based on the continuous signal model, which is used to analyze the system performance. In this block diagram it was used the sensor small signal model. The quantizer was linearized and modelled by a white noise source, $E(s)$, that was added to the sensor temperature, $T_s(s)$, which is a function of the fluid speed, $\vartheta(s)$. The unity gain block between sensor output and

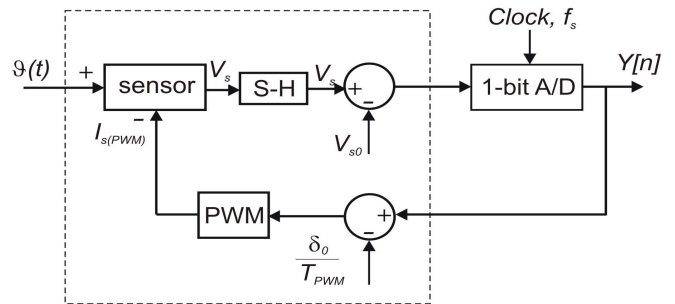


Figure 3. Block diagram of the pulsed current Σ - Δ modulator model.

the white noise source is used to transform the sensor temperature scale to the quantizer scale. The block $A_o(s)$ is a zero-order holder and ΔY_{so} is the squared current gain of the D/A converter in the Σ - Δ modulator feedback path. The sensor small signal model is described by:

$$T_s = \frac{1}{s-p} [K_\vartheta \vartheta(s) + K_{Y_s} Y_s(s)] \quad (7)$$

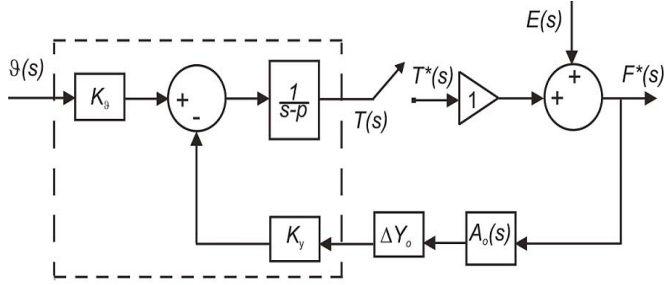


Figure 4. Block diagram used to analyze the system performance.

In which, $p = ((a+b\vartheta^2)S + \beta R_{so} Y_{so})/mc$ is the inverse of the sensor time constant, $k_\vartheta = b\vartheta^2 S(T_f - T_s)/mc$, and $k_y = R_{so}/mc$ are the coefficients associated to the fluid speed and to the sensor squared current Y_s , respectively. A zero-order holder, $A_o(s)$, transforms the modulator output samples to a continuous signal, with T as the oversampling period. $A_o(s)$ is given by:

$$A_o(s) = (1 - e^{-st})/s \quad (8)$$

With the model of the measurement system transfer function in the z-domain, it is possible to analyse the behaviour of the quantization noise frequency spectrum at the Σ - Δ modulator output and consequently the quantization in-band noise power in the Σ - Δ converter output. Finally, we can determinate the signal/noise relationship (SNR) and the effective resolution of the proposed measurement system.

B. Continuous Current System Transfer Function in the z-domain

The velocity step response for the mono-bit first-order Σ - Δ modulator with the thermoresistive sensor can be expressed by its z-domain transfer function as:

$$F(z) = \frac{z-r}{z-q} E(z) + \frac{z-r}{z-q} \quad (9)$$

where, r is the quantizer error transfer function zero and q is the system transfer function pole.

The quantizer noise (error) transfer function (NTF) has a zero that depends on the sensor small signal model pole p , for $r=e^{pT}$ with T being the oversampling period. The system transfer function pole q also depends on this parameter, and can be found as

$$q = \frac{k_y \Delta Y_{so}}{p} (1+r) + r.$$

The NTF zero degrades the noise attenuation in the signal band once there is a finite attenuation at DC frequency

instead of an infinite attenuation as in the ideal first-order sigma-delta modulator [7]. The frequency spectral density magnitude of the proposed measurement system quantization noise can be expressed by:

$$E_y(f) = \frac{E(f) \left(\sqrt{(1-r)^2 + 4r \sin^2\left(\frac{wT_s}{2}\right)} \right)}{\left(\sqrt{(1-q)^2 + 4q \sin^2\left(\frac{wT_s}{2}\right)} \right)} \quad (10)$$

The Σ - Δ converter output noise power signal band with a first order sensor, σ_{ey}^2 , in the frequency domain, is calculated from Σ - Δ modulator output noise spectral density, assuming that the modulator output signal has being filtered by an ideal filter on signal band frequency. The signal band noise power depends on the OSR and on the quadratic relationship involving the NTF zero and pole. Then:

$$\sigma_{ey}^2 = \int (E_y(f))^2 df = \frac{\sigma_{rms}^2 (1-r)^2}{OSR(1-q)^2} \quad (11)$$

C. Continuous Current System Measurement Resolution

To obtain the system theoretical resolution, the system noise power was compared to an N-bits Nyquist PCM noise power and the resolution, in number of bits, is given by (12). This expression shows the resolution dependence with OSR^{-1} and the quadratic relationship involving the NTF zero and pole.

$$N = -\frac{1}{2} \log_2 \left\{ \frac{1}{OSR} \frac{(1-r)^2}{(1-q)^2} \right\} \quad (12)$$

A better SNR can be obtained by increasing the modulator quantizer number of bits, by increasing the modulator order, or by limiting the input signal band under the sensor pole frequency. To verify the theoretical results, the pulsed current system was simulated in the time domain for a sine wave speed input. The system resolution is improved by half bit every time that the oversampling ratio is doubled.

IV. SIMULATION RESULTS

The sensor characteristics used in the theoretical analysis and in the system simulations were: $\beta = 0.000784 \text{ }^\circ\text{C}^{-1}$, $R_\theta = 102 \text{ } \Omega$, $S = 4 \times 10^{-9} \text{ m}^2$, $mc = 292 \times 10^{-12} \text{ J }^\circ\text{C}^{-1}$. The sensor temperature theoretical operation point was defined at $80 \text{ }^\circ\text{C}$ and the fluid speed range was defined from $\vartheta_{min} = 0$ to 20 m/s . The signal band frequency was chosen to be near system transfer function pole frequency, $f_B = 0.9 f_{sr}$. Simulations were made for the continuous current model using the developed analyses presented in the previous section, and are shown in Figures 5 to 7. Simulations for the pulsed current model, shown in Figure 3, were made and the results are compared

with continuous model results, as presented in Figure 8 and in Table 1.

Figure 5 shows the theoretical system output noise magnitude for the oversampling ratio equal to 256, zoomed into the signal band frequency. At DC there is a finite attenuation (-38.9 dB). This attenuation is -35.9 dB and -3 dB at the NTF zero and pole frequencies, respectively, which limit the system application in the signal band frequency.

Figure 6 shows the system NTF zero and pole locations in the z-plane.

Figure 7 shows theoretical system resolution, obtained from (12), as a function of the OSR. The system resolution is improved by half bit every doubling of the oversampling ratio.

To verify theoretical results the pulsed current system was simulated in the time domain for a sinusoidal fluid speed, expressed by (13), covering the full measurement range. The sine wave frequency was selected to be smaller than the sensor small model pole frequency.

$$\vartheta(t) = [10 + 10 \sin(\pi t / 10^5)] \text{ (m/s)} \quad (13)$$

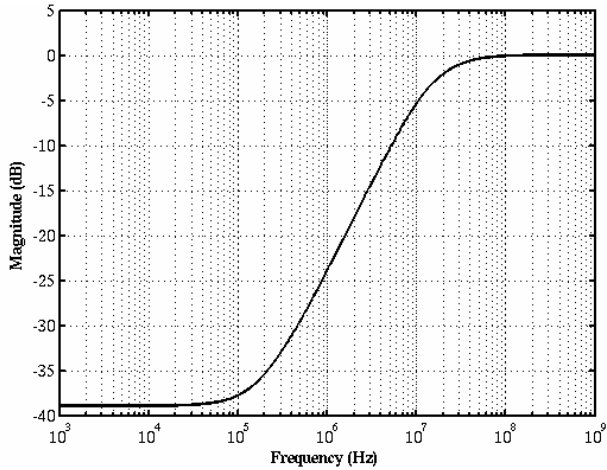


Figure 5. System noise transfer function magnitude.

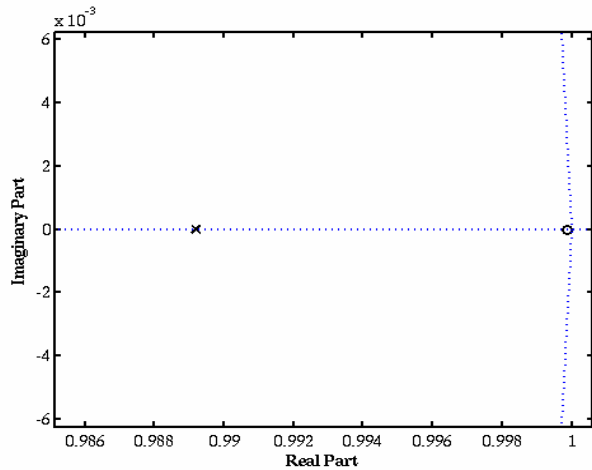


Figure 6. System NTF zero-pole located in z-plane.

The fluid speed was estimated, through simulation, from the data at the Σ - Δ modulator output, using a digital filter as presented in [8].

Figure 8 shows the estimated fluid speed absolute error for the pulsed current system, for the fluid speed full range of 20 m/s, and disregarding the dynamic resolution lost around the positive peak of the estimated fluid speed due to the fluid temperature mathematical compensation. These absolute errors are shown for the OSR equal to 64, 128 and 256.

The mean squared error for the pulsed current system was obtained from estimated fluid speed samples at the end of the converter, after the stabilization, and was calculated by

$$\sigma_{ey}^2 = \left(\frac{2}{\vartheta_{\max} - \vartheta_{\min}} \right)^2 \frac{1}{N_a} \sum_1^{N_a} [\vartheta_n(i) - \vartheta(i)]^2 \quad (14)$$

where N_a is the number of samples, ϑ_n is the estimated fluid speed at the output of the converter and ϑ is the fluid speed at the input of the converter.

The estimated fluid speed mean squared error was

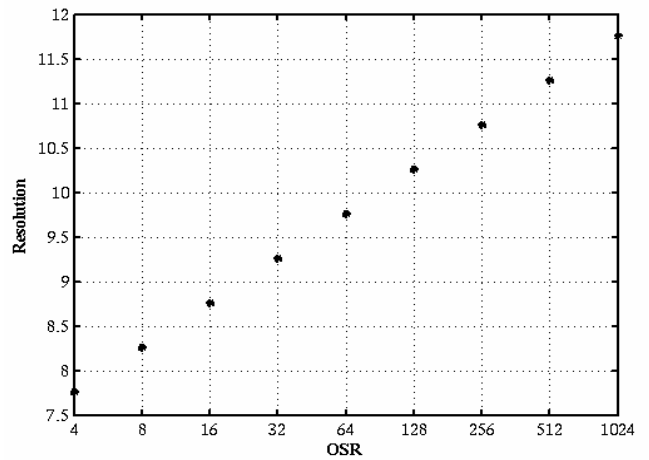


Figure 7. System resolution.

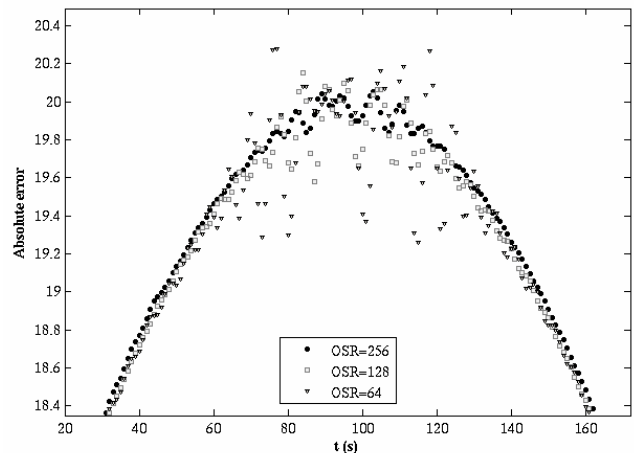


Figure 8. Pulsed current system: estimated absolute error.

compared with the N-bits Nyquist PCM noise power to obtain system resolution in time domain. The system resolution was given by equation (11):

$$N = -0.5 \log_2 \left\{ \frac{12}{(\vartheta_{\max} - \vartheta_{\min})^2} \frac{1}{N_a} \sum_1^{N_a} [\vartheta_n(i) - \vartheta(i)]^2 \right\} \quad (15)$$

Table 1 shows system resolution results obtained for three oversampling ratio values. The first column refers to system resolution results calculated from (12) and the two columns refer to the pulsed current system time domain simulation results that were calculated from (15). The pulsed current system resolution values are worst due to the uncompensated environment temperature, when comparing to theoretical system.

Table 1. Theoretical and Pulsed current systems simulated measurement resolution results.

OSR	Resolution (number of bits)	
	Theoretical System	Pulsed current System
64	9.7	6.4
218	10.2	7.3
256	10.7	8.2

V. CONCLUSION

The pulsed current fluid speed architecture presented here realized the expected A/D conversion with a lower resolution when compared to an ideal 1-bit Σ - Δ modulator. To obtain better measurement resolution, the input signal band frequency must be limited under sensor small signal transfer function pole frequency and the modulator output samples must be filtered at the sensor small signal pole frequency.

The pulsed current system SNR values are lower than for an ideal 1-bit Σ - Δ modulator, which is 1.5 bits for every doubling of the oversampling ratio.

This pulsed-current fluid speed measurement architecture does not need a 1-bit D/A converter in the feedback loop because this function is realized by PWM.

Fluid speed measurement system based on this same principle, with compensation of the environment temperature, will be our future objective.

VI. ACKNOWLEDGMENT

The authors wish to thank CAPES, CNPq, CAPES/COFECUB and FAPESQ/PRONEX for financial support and the award of fellowships during investigation period.

VII. REFERENCES

- [1] C. A. Leme, M. Chevroulet, H. Baltes, "A flexible architecture for CMOS sensor interfaces", Proceedings IEEE International Symposium on Circuits and Systems (ISCAS '92), pp. 1828-1831 May 1992
- [2] E. R. Riedijk, J. H. Huijsing, "A smart balanced thermal pyranometer using a sigma-delta A-to-D converter for direct communication with microcontrollers", Sensors and Actuators, pp. 16-25, volume 37-38, 1993.
- [3] A. Oliveira, L. S. Palma, A. S. Costa, R. C. S. Freire, A. C. C. Lima, "A Constant Temperature Operation Thermoresistive Sigma-Delta Solar Radiometer", 10th IMEKO TC7 International Symposium on Advances of Measurement Science, vol. 1, pp 199-204, June 2004.
- [4] R. C. S. Freire, G.S. Deep, C.C. Farias, Electrical equivalence solar radiometer configurations, in: Proc. XI Congresso Brasileiro de Automática, vol. 3, 1996, pp. 1249-1254.
- [5] L. S. Palma, A. Oliveira, A. S. Costa, R. C. S. Freire, A. C. C. Lima, A Constant Temperature Operation Thermoresistive Sigma-Delta Solar Radiometer. Proceedings 10th IMEKO, 2004. v. 1. p. 199-204.
- [6] A. Oliveira, L. S. Palma, A. S. Costa, R. C. S. Freire, A. C. C. Lima. A Constant Temperature Operation Thermo-Resistive Sigma Delta Transducer. In: Instrumentation and Measurement Technology Conference 2004, 2004, Como. Instrumentation and Measurement Technology Conference 2004, 2004. v. 3. p. 1175-1181.
- [7] J. C. Candy, G. C. Temes, Oversampling Methods for A/D and D/A Conversion, cap: Introduction, Oversampling Delta-Sigma Data Converters Theory, Design and Simulation, IEEE Press, pp. 1-25.
- [8] S. Park, "Principles of Sigma-Delta Modulation for Analog-to-Digital Converters". Motorola DSP: Strategic Applications and Digital Signal Processor Operation, Motorola, 1998.